



HAL
open science

Landscape spatial configuration influences phosphorus but not nitrate concentrations in agricultural headwater catchments

Rémi Dupas, Antoine Casquin, Patrick Durand, Valérie Viaud

► **To cite this version:**

Rémi Dupas, Antoine Casquin, Patrick Durand, Valérie Viaud. Landscape spatial configuration influences phosphorus but not nitrate concentrations in agricultural headwater catchments. *Hydrological Processes*, 2023, 10.1002/hyp.14816 . hal-03953928

HAL Id: hal-03953928

<https://hal.inrae.fr/hal-03953928>

Submitted on 24 Jan 2023

HAL is a multi-disciplinary open access archive for the deposit and dissemination of scientific research documents, whether they are published or not. The documents may come from teaching and research institutions in France or abroad, or from public or private research centers.

L'archive ouverte pluridisciplinaire **HAL**, est destinée au dépôt et à la diffusion de documents scientifiques de niveau recherche, publiés ou non, émanant des établissements d'enseignement et de recherche français ou étrangers, des laboratoires publics ou privés.

1 **Landscape spatial configuration influences phosphorus but not nitrate**
2 **concentrations in agricultural headwater catchments**

3 Rémi Dupas ¹, Antoine Casquin ², Patrick Durand ¹, Valérie Viaud ¹

4 ¹ INRAE, UMR SAS 1069, L'Institut Agro, Rennes, France

5 ² Sorbonne Université - UPMC, UMR METIS, Paris, France

6

7 **Corresponding Author:** Rémi Dupas, remi.dupas@inrae.fr

8

9 **Abstract**

10 Landscape organized (or structured) heterogeneity influences hydrological and biogeochemical patterns
11 across space and time. We developed landscape indices that describe the spatial configuration of nutrient
12 sources and sinks as a function of their hydrological distance to the stream (lateral dimension) or to the
13 outlet (longitudinal dimension) and their intersection with flow-accumulation areas. Using monthly
14 nitrate, total phosphorus (TP), soluble reactive phosphorus (SRP) and daily discharge (Q) data from 221
15 rural catchments (1-300 km²) from 2010-2020, we observed higher variability in flow-weighted mean
16 concentrations in smaller catchments than in larger ones. The variability in landscape configurations
17 also decreased with increasing catchment size. A landscape configuration index, calculated as mean
18 arable land use weighted by spatial data on hydrological distance and flow accumulation, improved
19 prediction of TP and SRP, but not nitrate, compared to the unweighted mean arable land use. We
20 conclude that landscape configuration influences phosphorus transfer more than nitrate transfer, and that
21 flow-accumulation zones and riparian areas are critical source areas for TP and SRP, respectively. By
22 contrast, landscape spatial configuration in the lateral (upslope-downslope) and longitudinal (upstream-
23 downstream) dimensions did not have an identifiable influence on nutrients temporal dynamics. The
24 indices developed in this study can help design landscapes that minimize diffuse phosphorus losses to
25 streams and show that landscape management is not a first order control for nitrate losses.

26 **Keywords:** landscape; catchment; nutrient; agriculture; nitrate; phosphorus

27

28 **1. Introduction**

29 Landscape spatial organization is often assumed to influence hydrological and biogeochemical patterns
30 across space and time. Topography drives the spatio-temporal dynamics of water flowpaths and
31 residence times (Beven and Kirkby, 1979). Topography also influences the spatial arrangement of
32 landscape elements (e.g. agricultural fields, buffer strips, hedgerows, ditches) that can act as sources or
33 sinks for different forms of soluble and particulate nitrogen and phosphorus (P). The spatial arrangement
34 of polygonal, linear or punctual landscape elements is called landscape spatial configuration. Interacting
35 influences of topography on hydrological and landscape patterns thus result in spatially organized
36 patterns in biogeochemical processes, including processes such as nutrient mobilization, retention or
37 removal (Bernhardt et al., 2017; Covino et al., 2022; Krause et al., 2017).

38 Knowledge of topography-driven patterns in hydrological and biogeochemical hotspots at the catchment
39 scale can help design landscapes that minimize nutrient losses to streams while maintaining an
40 acceptable level of agricultural production (Casal et al., 2018; Doody et al., 2016; McDowell et al.,
41 2014). This includes the use of techniques for mapping critical source areas (CSA) (i.e. areas where
42 most diffuse pollution originates, and hence outside of which landscape elements considered as nutrient
43 sources should be placed) and optimal placement of buffer zones (Dorioz et al., 2006; Schoumans et al.,
44 2014).

45 Topographic indices derived from Digital Elevation Models (DEM) are often used to locate these areas
46 (e.g. Djodjic and Villa (2015); Lane et al. (2009)). High uncertainties still exist in delineating CSAs, as
47 validating them relies on walkover surveys of observable features such as erosion marks, which are
48 tedious to perform (Reaney et al., 2019). Several studies have attempted to evaluate “expert-based” CSA
49 delineation with water-quality data across contrasting catchments, but they often relied on few
50 catchments (Djodjic and Markensten, 2019; McDowell and Srinivasan, 2009; Shore et al., 2014; Thomas
51 et al., 2016). As an alternative, “data-driven” methods can assess the influence of landscape spatial
52 configuration on nutrient export (Casquin et al., 2021; Peterson et al., 2011; Van Sickle and Johnson,
53 2008). These methods use one or several topographic indices as weighting functions of a land-use class
54 considered as a nutrient source (typically agriculture or arable land use) to assess whether a topography-

55 weighted land-use percentage predicts nutrient concentrations better than an unweighted land-use
56 percentage. A significant improvement in predicting them for a large number of catchments is
57 interpreted as landscape spatial configuration influencing nutrient losses, and the topography-weighted
58 function can be used to delineate CSAs (Casquin et al., 2021). Such topographic indices typically
59 combine flow-distance metrics, either to the stream or to the outlet, and flow-accumulation metrics
60 (Peterson et al., 2011; Staponites et al., 2019, Zampella et al., 2007) and may involve one or more
61 calibrated coefficients (Casquin et al., 2021; Van Sickle and Johnson, 2008; Walsh and Webb, 2014).

62 The influence of landscape structured heterogeneity on biogeochemical and hydrological processes may
63 also influence the temporal dynamics of nutrient concentrations, which are important to consider when
64 evaluating ecological impacts (Bol et al., 2018; Stamm et al., 2014). According to the concept of
65 hydrological connectivity, different parts of catchments contribute differently depending on flow
66 conditions: during the high-flow season or a runoff event, shallow flowpaths become active, while the
67 contribution to flow of areas distant from the river network or located most upstream increases (Jencso
68 et al., 2009; Zimmer and McGlynn, 2018). These three components of connectivity are termed vertical
69 (shallow vs deep), lateral (upslope vs downslope) and longitudinal connectivity (upstream vs
70 downstream). Using a physically-based parsimonious model, Musolff et al. (2017) showed that a major
71 driver of dilution, enrichment and constant concentration-discharge patterns (a metric of concentration
72 temporal dynamics) was structured heterogeneity of sources in relation to their hydrological distance to
73 the outlet. Their virtual experiments, however, did not identify which dimension of structured
74 heterogeneity (vertical, lateral or longitudinal) in source gradients were the most influential. Most
75 studies interpreting concentration-discharge relationships as a function of structured heterogeneity of
76 sources focus on the vertical dimension, and several of them support this hypothesis with data (e.g.
77 Botter et al. (2020); Ebeling et al. (2021b); Stewart et al. (2022)). Others have assumed an influence of
78 lateral gradients in sources on concentration temporal dynamics, such as when land use intensity in the
79 riparian zone differs from that in the upslope part of the catchment (Musolff et al., 2021; Strohmenger
80 et al., 2021), or an influence of longitudinal gradients, such as when land use and/or hydrology in

81 upstream sub-catchments differ from those in the downstream part of the catchment (Dupas et al., 2021;
82 Winter et al., 2021).

83 The research question of the present study was: Does the landscape spatial configuration influence
84 nutrient concentrations and dynamics in headwater streams? To address this question, we i)
85 characterized the landscape spatial configuration in 221 headwater catchments (i.e. the spatial
86 configuration of arable land in the lateral and longitudinal dimension); ii) analysed correlations between
87 a landscape configuration index and flow-weighted mean concentrations of nitrate, soluble reactive P
88 (SRP) and total P (TP); and iii) explored relationships between indices of landscape spatial configuration
89 and the slope of the concentration-discharge relationship.

90 Nitrate, SRP and TP are the nutrients most commonly monitored in regulatory surveillance programmes
91 for the European Union Water Framework Directive, due to their role as factors that control
92 eutrophication (Le Moal et al., 2019). The study area encompasses the Brittany region, western France,
93 where a large number of small (<300 km²) and independent headwater catchments are monitored
94 monthly using the same protocol (Guillemot et al., 2021). The study area spans large gradients in land
95 use, topography, annual runoff (section 2.1.) and has high variability in nutrient concentration dynamics,
96 but no large discontinuities in physiographic properties as would occur if using a national or continental
97 database (Frei et al., 2020). Such discontinuities (e.g. contrasting geology) would influence nutrient
98 concentration dynamics greatly and potentially mask the effect of the landscape spatial configuration
99 that we wanted to distinguish (Dupas et al., 2020; Guillemot et al., 2021). Finally, the contribution of
100 diffuse agricultural pollution to nutrient loads is particularly high in this region (Legeay and Gruau,
101 2014).

102 **2. Material and methods**

103 **2.1. River monitoring data**

104 The study area of Brittany (27,000km², Figure S1) is located in the Armorican Massif, which consists
105 mainly of igneous and metamorphic rocks (schist, micaschist, granite, Fig S2), and has a relatively flat
106 topography with elevation ranging from 0-385 m above sea level. The area has a temperate oceanic
107 climatic, with mild temperatures (12°C on average) and a rainfall gradient of 700-1300 mm from east

108 to west. Its hydrology is driven mainly by the dynamics of shallow groundwater that develops in the
109 weathered rock aquifer. It has a marked seasonality, the hydrologically effective rainfall being the
110 highest in winter. Overland flow is moderate and generated mainly in saturated areas. The wet conditions
111 and relatively impervious bedrock lead to a high river density given the temperate oceanic climate (1
112 km.km⁻¹), and to the development of hydromorphic soils along the riparian zone that cover nearly 20%
113 of the land area (Berthier et al., 2014). Agriculture represents 60% of the land use and is particularly
114 intensive due to the regional specialization in mixed crop-livestock farming with high livestock
115 densities. Previous studies have shown that diffuse agricultural sources represent >95% of nitrate and
116 *ca.* 70% of P loads in rivers (Dupas et al., 2013; Legeay and Gruau, 2014).

117 We selected 221 independent headwater catchments (1-300 km², table S1) in which water quality was
118 monitored as part of the EU Water Framework Directive, and made publically available via
119 <https://naiades.eaufrance.fr/>. The water-quality parameters studied here were nitrate, SRP and TP. As
120 water quality was typically monitored on a monthly basis, we calculated water-quality metrics when at
121 least 40 concentration data points were available during the 2010-2020 study period. This selection
122 criterion resulted in 221, 186 and 185 catchments for nitrate, SRP and TP, respectively. Because existing
123 discharge monitoring stations in Brittany are not necessarily located at the water-quality monitoring
124 points, we used the geomorphology-based SIMFEN model to estimate daily discharge at the outlet of
125 each of our study catchments (de Lavenne and Cudennec, 2019). Developed for Brittany, SIMFEN
126 predicts discharge in ungauged catchments by transposing hydrographs from neighbouring gauged
127 ‘donor’ catchments by convoluting a “net rainfall” (i.e. the water flowing through the hillslope-river
128 interface) through the river network of the ungauged catchments (de Lavenne and Cudennec, 2019).

129 The metrics used to describe nutrient concentrations and dynamics were the flow-weighted mean
130 concentration (FW-nitrate, FW-SRP, FW-TP), the slope of the linear log(concentration)-log(discharge)
131 relationships and the ratio of the coefficient of variation of concentration to that of discharge (CVratio).
132 Concentrations were calculated as flow-weighted means rather than ordinary arithmetic means to
133 increase the contribution of data points during high-flows (when diffuse sources are dominant) and
134 decrease the contribution of data points during low-flows (when point sources and in-stream processes

135 may play a larger role). The slope of the linear log(concentration)-log(discharge) relationship and the
136 CVratio are commonly used variables to characterize nutrient export regimes and export patterns
137 (Musolff et al., 2015; Liu et al., 2022).

138 **2.2.Landscape indices**

139 We used two categories of landscape indices, to assess the influence of landscape spatial configuration
140 on mean nutrient concentrations and seasonal dynamics. The first was the landscape configuration index
141 (Casquin et al., 2021; Peterson et al., 2011), which aims to predict flow-weighted mean concentrations
142 of nitrate, TP and SRP as a function of the distance of their sources to the stream and their intersection
143 with flow-accumulation zones. The second category of landscape indices consisted of two metrics that
144 describe the spatial configuration of nutrient sources in the lateral (upslope-downslope) and longitudinal
145 (upstream-downstream) dimensions. The lateral and longitudinal configuration indices aim to test the
146 hypothesis that the spatial arrangement of sources in those dimensions influences nutrient dynamics.
147 For both categories of landscape indices, we considered the configuration of arable land as a nutrient
148 source, as we selected study catchments in which diffuse agricultural contamination is the dominant
149 source of contamination in rivers (Guillemot et al., 2021).

150 The landscape configuration index (LCI) was calculated as a single value for each catchment, as a
151 weighted-mean percentage of arable land use. The weighting function is a topographic index that
152 combines two variables derived from a DEM and two coefficients to optimize (a and b):

$$153 \quad LCI(a, b) = \frac{\sum_i \left(\frac{Flowacc_i^a}{LatDistance_i^b} * arable_i \right)}{\sum_i \frac{Flowacc_i^a}{LatDistance_i^b}} \quad [1]$$

154 where, for each pixel “i” in a given catchment, “flowacc_i” is the flow accumulation (i.e. the drainage
155 area of each grid cell), “LatDistance_i” is the hydrological distance to the stream and “arable_i” is 1 if the
156 land-use type is arable or 0 if not. For (a=0, b=0), the index equals the percentage of arable land-use,
157 while for (a=1, b=0) or (a=0, b=1) it equals the percentage of arable land-use weighted by “flowacc”
158 alone or “1/LatDistance” alone, respectively.

159 We varied a and b to maximize the Spearman's rank correlation between LCI(a,b) and the flow-weighted
 160 mean nitrate, TP and SRP concentrations of the study headwaters. We varied a from 0-6 and b from 0-
 161 8, with an increment of 0.1. We restricted the exploration space for a and b so that the weight of the top
 162 5% of pixels could not exceed 95% of the total weight in the region. This avoided finding optimal
 163 coefficient values that would correspond to an unrealistic situation in which only a few pixels would
 164 contribute nearly all the nutrient flux. This approach resulted in 4941 calculations of LCI(a, b), of which
 165 2169 met the latter condition and whose correlations with the flow-weighted mean concentrations were
 166 analysed. We considered that landscape spatial configuration had an influence if it predicted flow-
 167 weighted mean concentrations better than the land use composition did (i.e. if at least one pair (a, b)
 168 resulted in $LCI(a,b) > LCI(0,0) + 0.1$). We then examined the top 50 optimal (a, b) to assess the relative
 169 influence of flow accumulation and hydrological distance to the stream in determining CSAs. When
 170 successfully calibrated, the LCI weighting function $\sum_i \frac{Flowacc_i^a}{LatDistance_i^b}$ can be used as a nutrient export risk
 171 map and we considered pixels above the 90th percentile of this function to represent CSAs.

172 The lateral and longitudinal configuration indices were calculated as a single value for each catchment
 173 as follows:

$$174 \quad LatIndex = \frac{\sum_i \left(\frac{1}{LatDistance_i} * arable_i \right)}{\left(\sum_i \frac{1}{LatDistance_i} \right) * mean(arable_i)} \quad [2]$$

$$175 \quad LongIndex = \frac{\sum_i \left(\frac{1}{LongDistance_i} * arable_i \right)}{\left(\sum_i \frac{1}{LongDistance_i} \right) * mean(arable_i)} \quad [3]$$

176 where, for each pixel "i" in a given catchment, the variables "LatDistance_i" and "arable_i" are the same
 177 as in [1] and "LongDistance_i" is the longitudinal distance from the entry point to the stream to the
 178 catchment outlet. Because of the normalization by mean(arable), LatIndex >1 indicates that arable fields
 179 are located more downslope, i.e. near the stream network, while LatIndex <1 indicates that arable fields
 180 are located more upslope. Similarly, LongIndex >1 indicates that arable fields are located more
 181 downstream, i.e. near the catchment outlet, while LongIndex <1 indicates that arable fields are located

182 more upstream. We analyzed correlations between LCI(a, b) and the flow-weighted mean concentrations
183 of nitrate, SRP and TP to address research objective (ii), and we analyzed correlation between LatIndex,
184 LongIndex and the log(concentration)-log(discharge) slopes to address research objective (iii).

185 **2.3. GIS processing**

186 Calculating the landscape indices requires a DEM raster, a map of arable land use and a river network.
187 We generated the spatial data necessary to calculate the indices using ArcGis 10.8 (ESRI, 2021) and we
188 performed the raster calculations in R (R Core Team, 2021).

189 We used a 25 m resolution DEM (BD ALTI, IGN 2018) that served as a reference layer for the
190 rasterization and alignment of the river network and arable land-use data. The river network data came
191 from the BD TOPAGE (IGN, 2021), while the reference spatial data for France and the arable land-use
192 data came from the national Land Parcel Identification System (LPIS). In the LPIS, each parcel
193 identified as arable at least once from 2010-2020 was assigned a value of arable = 1 and the rest arable
194 = 0. Thus, agricultural land cover classes such as permanent grassland and orchards were not considered
195 as sources, but temporary grassland in rotation with row crops was. This binary classification of land-
196 use types may appear arbitrary, but attributing intermediate values to multiple land cover types would
197 require strong assumptions about their respective influence on nutrient export or a computation-
198 intensive calibration step. Furthermore, previous studies in the same region found a stronger correlation
199 between nutrient concentrations and arable land use than total agricultural land use (Guillemot et al.,
200 2021).

201 The DEM was hydrologically corrected by ‘filling’ depressions on hillslopes and ‘burning’ the river
202 network. We used a multiple flow direction algorithm (Qin et al., 2007) to determine flow accumulation
203 (log-transformed) and the flow distances. In the ArcGis 10.8 ‘Spatial analyst/Hydrology’ toolbox, we
204 used ‘Flow Distance’ to calculate LatDistance and the difference between the outputs of ‘Flow Distance’
205 and ‘Flow Length’ to calculate LongDistance. To calculate the landscape indices in R, we assigned the
206 value ‘NA’ to pixels that intersected the river network.

207 **3. Results and discussion**

3.1. Variability in nutrient concentration dynamics and landscape spatial configuration

The 221 study catchments spanned a wide range of flow-weighted mean nutrient concentrations: nitrate ranged from 3.0-61.1 mg.l⁻¹ (mean=29.5mg.l⁻¹), SRP ranged from 0.01-0.33 mg.l⁻¹ (mean=0.05mg.l⁻¹) and TP ranged from 0.1-0.39 mg.l⁻¹ (mean=0.13mg.l⁻¹). SRP represented 16-82% of TP (mean=37%).

Flow-weighted mean concentrations had a higher variability in smaller catchments than in larger ones (Figure 1). Previous studies have identified the same spatial trend in Brittany (Abbott et al., 2018a; Gu et al., 2021) as well as elsewhere (e.g. Shogren et al. (2019)). This could be because smaller catchments may capture the extreme conditions in the study area (related to nutrient source inputs, retention potential or landscape spatial arrangement), while larger catchments tend to be more representative of average conditions in the region. While the recent study of Guillemot et al. (2021) identified that land use (along with the climate, topography and soil type) could explain part of the variability observed, the present study specifically investigated the influence of landscape spatial configuration on concentrations (section 3.2) and concentration dynamics (section 3.3).

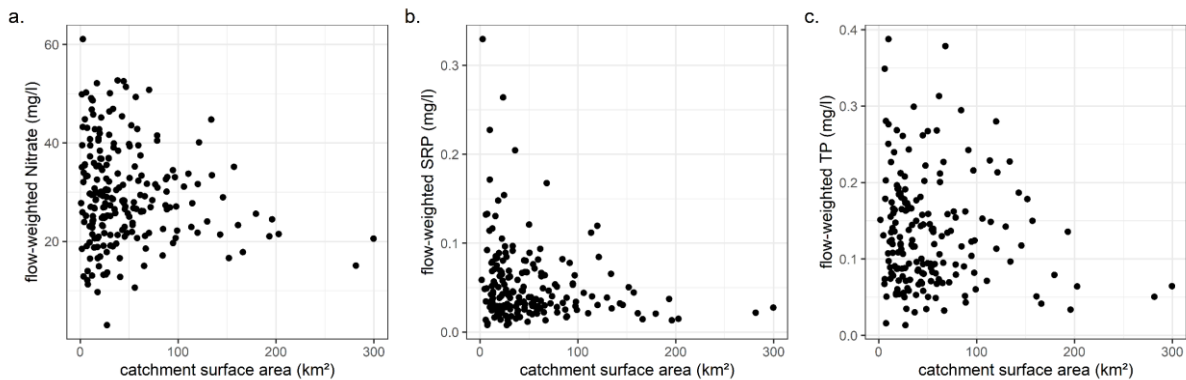
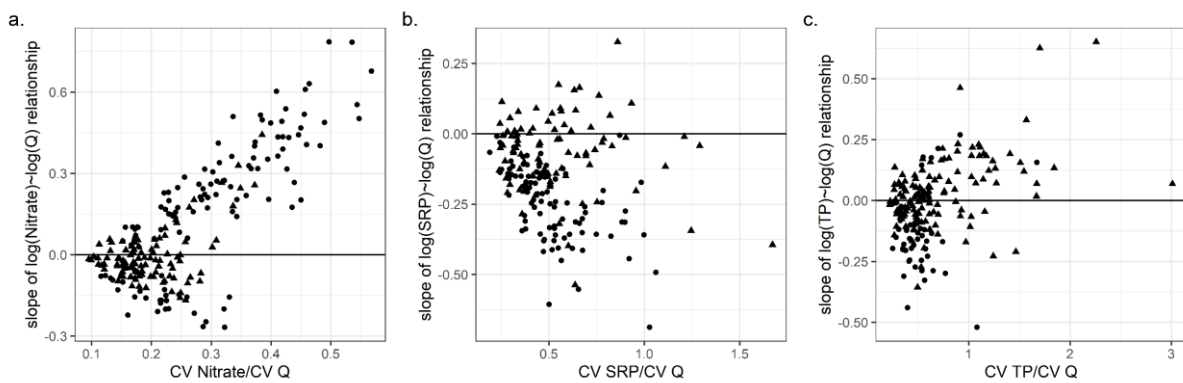


Figure 1. Relationships between catchment size and flow-weighted mean concentrations of (a) nitrate, (b) soluble reactive phosphorus (SRP) and (c) total phosphorus (TP) in 221 headwater catchments in Brittany (2010-2020).

The CV ratio was <1 for 100%, 98% and 96% of the catchments for nitrate, SRP and TP respectively. It was <0.5 for 98%, 53% and 43% of the catchments for nitrate, SRP and TP respectively. The lower variability in concentrations compared to that of discharge, often called chemostasis, is commonly

229 observed for many solutes and catchment types (Godsey et al., 2019; Musolff et al., 2015; Thompson et
230 al., 2011), especially in intensive agricultural catchments with large amounts of legacy nutrients in the
231 soil and groundwater (Basu et al., 2010).

232 For the statistically significant (p -value <0.05) C-Q relationships, the slope was positive for nitrate in
233 most of the catchments (73%), negative for SRP in all catchments and negative for TP in most of the
234 catchments (86%). Slopes were non-significant in 48%, 47% and 76% of the catchments for nitrate, SRP
235 and TP, respectively. There were strong correlations between the C-Q slope and CV ratio for nitrate
236 (positive for positive C-Q slopes and negative for negative C-Q slopes), while relationships between the
237 C-Q slope and CV ratio were less clear for SRP and TP (Figure 2).

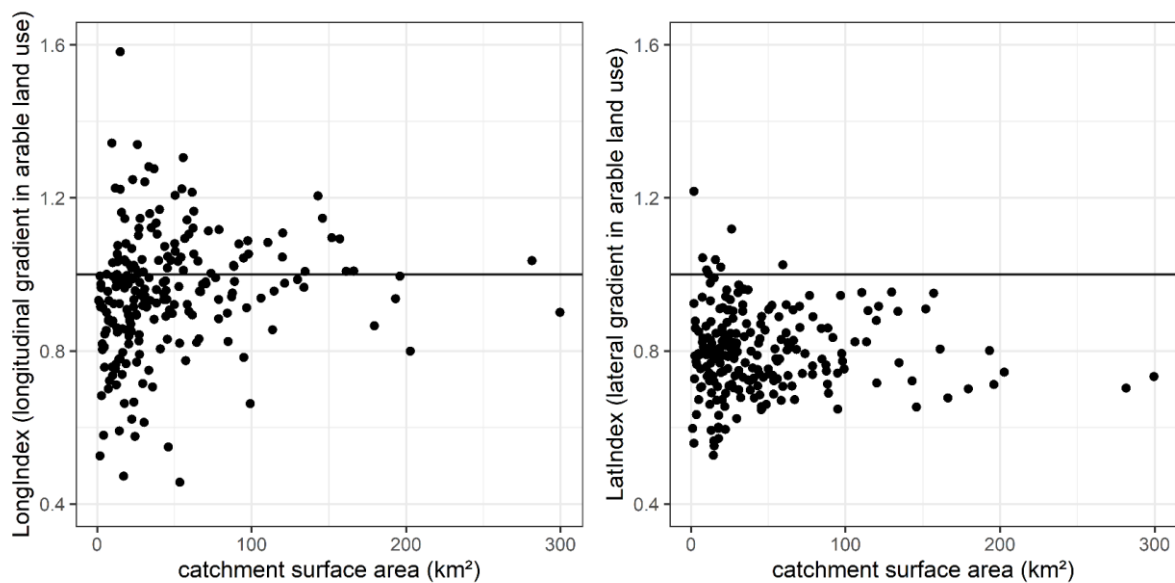


238

239 **Figure 2. Relationships between the coefficient of variation (CV) ratio and concentration-**
240 **discharge (C-Q)-slope for (a) nitrate, (b) soluble reactive phosphorus (SRP) and (c) total**
241 **phosphorus (TP) in 221 headwater catchments in Brittany (2010-2020). Round dots indicate**
242 **significant C-Q slope ($p < 0.05$) and triangular dots non-significant C-Q slopes ($p > 0.05$).**

243 The most common pattern identified in temperate catchments is a dominance of positive C-Q slopes for
244 nitrate and negative slopes for SRP and TP (Betton et al., 1991; Ebeling et al., 2021a). Minaudo et al.
245 (2019) and Musolff et al. (2021) showed that seasonal variations predominantly influenced these
246 patterns captured with low frequency data. Analysis of high-frequency data in Brittany showed that
247 nitrate is higher and P lower during the winter high-flow season, despite the prevalence of dilution
248 patterns for nitrate and accretion patterns at the scale of storm events (Fovet et al., 2018). The large
249 percentage of non-significant slopes may have been due to this contrasting influence of flow at seasonal

250 and event time scales (Minaudo et al., 2019; Moatar et al., 2017). The existence of negative C-Q patterns
251 for nitrate in contexts of a dominant diffuse source was previously documented in Brittany, but the
252 factors that control them remain unclear (Guillemot et al., 2021; Martin et al., 2004; Ruiz et al., 2002).
253 In the literature, C-Q patterns are generally interpreted in terms of i) dominance of point versus diffuse
254 sources (Abbott et al., 2018b; Ehrhardt et al., 2021; Van Meter et al., 2020); ii) heterogeneity in nutrient
255 sources and temporally variable hydrological connectivity, especially in the vertical dimension (Botter
256 et al., 2020; Ruiz et al., 2002; Zarnetske et al., 2018) and iii) biogeochemical processes in- and near-
257 stream, which may remove nitrate and retain/remobilize P forms (Casquin et al., 2020; Lutz et al., 2020).
258 Like for flow-weighted mean concentrations, we observed higher variability in LatIndex and LongIndex
259 in smaller catchments than in larger ones (Figure 3). Most LatIndex values were <1 , indicating that
260 arable fields were preferentially located upslope. This spatial distribution of arable fields was expected,
261 as valley bottoms typically consist of less productive hydromorphic soils in Brittany, while hillslopes
262 are more suitable for arable crops and intensive temporary grassland (Frei et al., 2020). LongIndex
263 values were equally distributed on both sides of the $y=1$ line, indicating no general trend in the
264 distribution of arable land in the longitudinal dimension, but a high variability in situations, especially
265 in the smaller catchments. This confirms observations made in other studies (e.g. Bishop et al. (2008);
266 Bol et al. (2018); Gu et al. (2021)) that studying small headwaters is key to increasing the variability in
267 catchment conditions when statistically analysing water-quality and catchment attributes such as
268 landscape indices. For this reason, we limited the analysis of correlations between water-quality metrics
269 and landscape indices to sub-catchments smaller than 50 km², leaving 148 of the 221 catchments for
270 subsequent analyses. Using a threshold of *ca.* 50 km² to study relationships between water-quality
271 metrics and landscape indices is also justified by the increasing influence of in-stream processes in larger
272 catchments, which may significantly alter nutrient concentrations and dynamics (Casquin et al., 2020).
273 Finally, a threshold of *ca.* 50 km² to analyze headwater variability is consistent with previous work
274 throughout Europe (Bol et al., 2018; Djodjic et al., 2021).



275

276 **Figure 3. Relationships between catchment size and LatIndex and LongIndex. LatIndex >1**
 277 **indicates arable fields preferentially located downslope (i.e. near the stream network), while**
 278 **LatIndex <1 indicates arable fields preferentially located upslope. LongIndex >1 indicate arable**
 279 **fields preferentially located downstream (i.e. near the catchment outlet), while LongIndex <1**
 280 **indicates arable fields preferentially located upstream.**

281 **3.2. Relationships between the Landscape configuration index and flow-weighted**
 282 **mean nutrient concentrations**

283 The percentage of arable land use (i.e. the value of LCI(0,0)) had a stronger rank correlation with flow-
 284 weighted mean nitrate concentration ($r=0.74$) than with SRP ($r=0.27$) and TP ($r=0.40$). A stronger
 285 correlation between land-use composition metrics and nitrate concentrations compared to P forms is
 286 common in statistical analyses of catchment data (Guillemot et al., 2021; Minaudo et al., 2019). Several
 287 potential reasons have been suggested: i) estimated mean P concentrations have a higher uncertainty
 288 than those of nitrate concentrations, hence mean P concentrations are more difficult to predict with
 289 catchment descriptors than mean nitrate concentrations; ii) point sources of pollution represent a larger
 290 percentage of P export than nitrate export, hence a proxy of diffuse agricultural sources alone cannot
 291 accurately predict P; iii) P is subjected to more complex and spatially variable retention processes than
 292 N, and landscape spatial configuration is one of the factors that control landscape P retention. The LCI

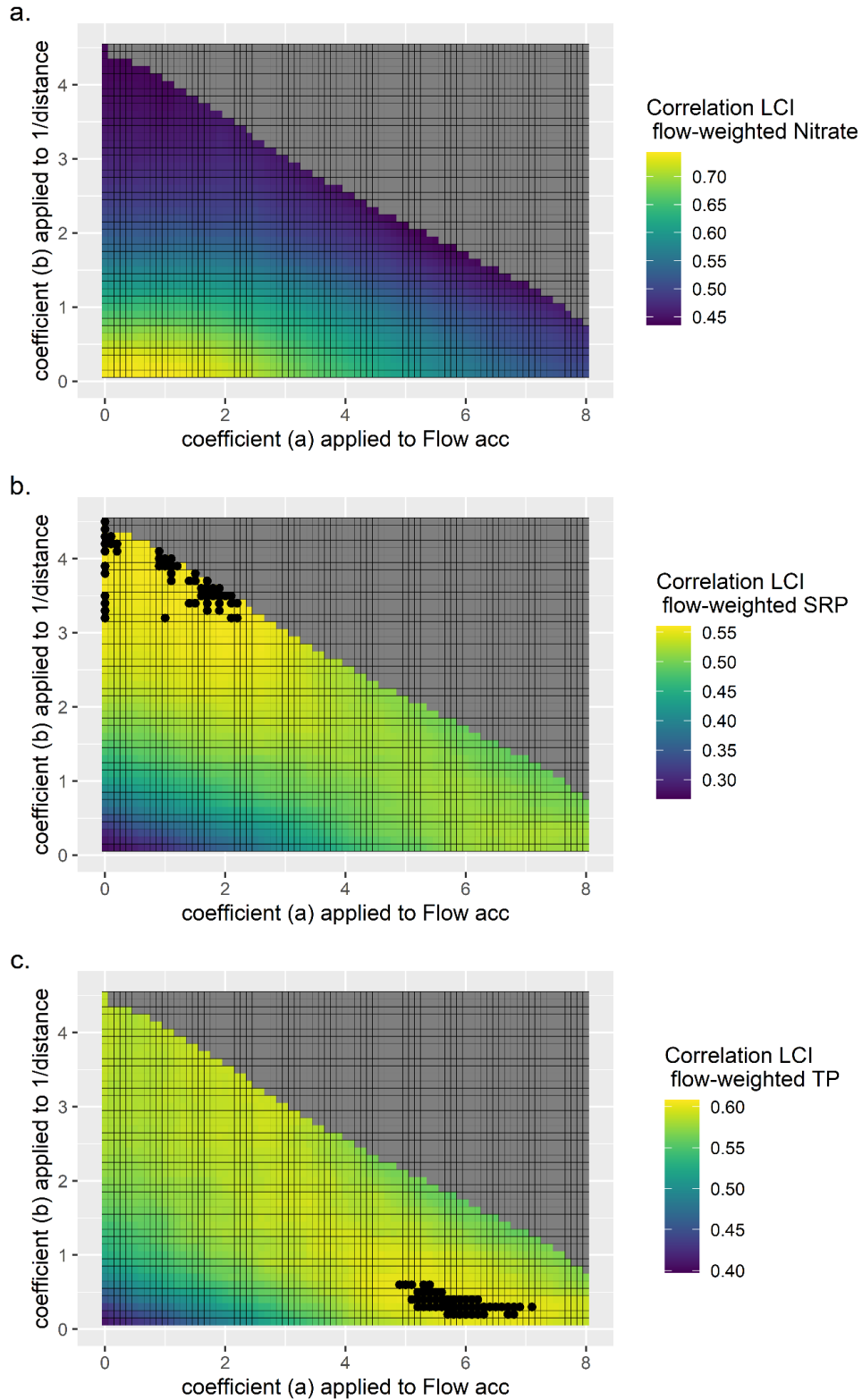
293 aimed to test the latter hypothesis by identifying whether (a,b) pairs exist for which
294 $LCI(a,b) > LCI(0,0) + 0.1$.

295 Varying the coefficients a and b did not substantially (>0.1) improve the correlation between $LCI(a,b)$
296 and flow-weighted mean nitrate concentration, but did improve its correlation with flow-weighted mean
297 SRP and TP, by +0.29 and +0.21, respectively. We interpret this result as indicating that landscape
298 spatial configuration influences the export of P more than that of nitrate. This does not mean that
299 landscape management is irrelevant for reducing nitrate transfer, as other studies have demonstrated an
300 effect (Casal et al., 2018; McDowell et al., 2014). Instead, it could mean that the effect is too small to
301 be detected with our method or that relevant landscape configurations that maximize N retention should
302 consider factors besides those included in the LCI. Our method also may not have detected an influence
303 of landscape configuration on nitrate because the landscape configurations that actually minimize N
304 losses did not occur in the study catchments, or the binary classification of land-use types into sources
305 or sinks was too simplistic. We think, however, that using intermediate source/sink values instead of the
306 binary approach would result in indetermination problems and obscure the influence of landscape
307 configuration in the LCI. The lack of a significant influence of landscape spatial configuration on nitrate
308 transfer is consistent with knowledge on its main transfer pathway via groundwater, which frequently
309 bypasses landscape buffers that may be present on the surface (Guillemot et al., 2021; Ruiz et al., 2002).

310 The optimal (a,b) pairs for predicting flow-weighted mean SRP and TP were (1.9, 3.6) and (5.7, 0.3),
311 respectively, and the top 50 pairs were located in the same area of parameter space for each parameter
312 (Figure 4). These optimal values differed from (a=0, b=0), (a=0, b=1), (a=1, b=0) or (a=1, b=1), which
313 shows that, compared to previous landscape indices calculated as arable land weighted by flow
314 accumulation alone, inverse distance to the stream alone or their ratio (Peterson et al., 2011; Staponites
315 et al., 2019, Zampella et al., 2007), the addition of calibrated coefficients (a, b) as power-law coefficients
316 improved prediction of TP and SRP. Both distance to the stream and flow-accumulation influenced SRP
317 and TP, as also determined by Casquin et al. (2021) in 19 headwaters in Brittany. Thus, current
318 regulations that consider only the distance to river networks to restrict certain agricultural practices or
319 encourage the establishment of buffer zones (e.g. the European Nitrate directive and Water Framework

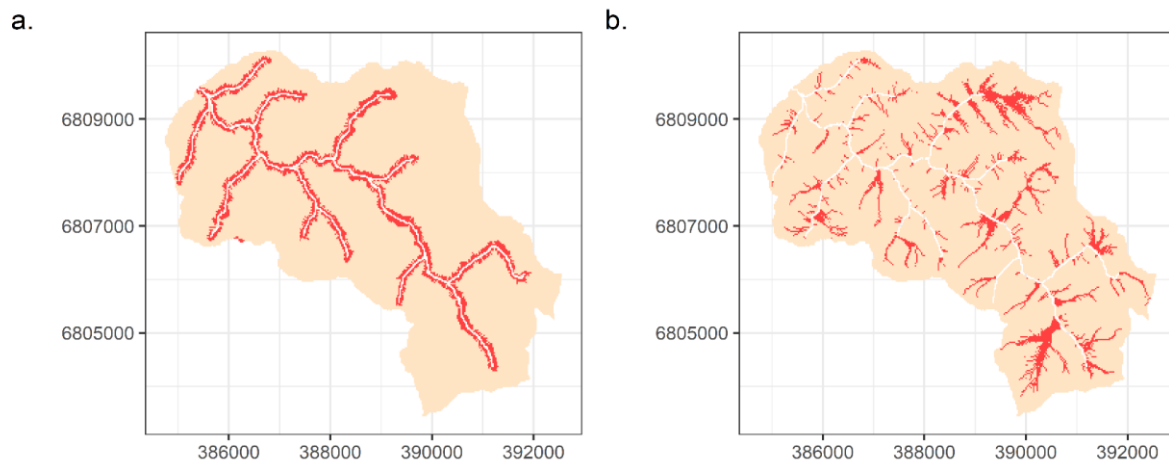
320 directive) could be refined by considering flow-accumulation information as well. The optimal (a,b)
321 pairs for predicting TP and SRP showed greater influence of flow accumulation or distance to the stream,
322 respectively. The combined effect of both types of topographic data, but a different predominant type
323 for TP and SRP, was clearly visible in a CSA map created from the >90th percentile of the LCI weighting
324 function (Figure 5). Greater influence of distance to the stream for SRP and flow-accumulation for TP,
325 which comprises a majority of particulate P (Dupas et al., 2015), is consistent with current knowledge
326 on their respective transfer mechanisms. Soluble reactive P is transferred mainly via subsurface
327 groundwater pathways or runoff on water-saturated soils (i.e. in the riparian zone where the shallow
328 groundwater can intersect the soil surface during wet periods) (Bol et al., 2018; Dupas et al., 2017; Gu
329 et al., 2017; Mellander et al., 2015). Particulate P, on the other hand, is more susceptible to transfer via
330 concentrated erosion processes, which is more likely to occur in flow-accumulation areas (Pionke et al.,
331 1999; Reaney et al., 2019). The two P forms, however, are not independent, because particulate forms
332 can transform into to soluble forms (and vice-versa) along the transport continuum from soils to streams
333 and rivers (Bol et al., 2018; Casquin et al., 2020; Gu et al., 2017). Fig S3 shows an optimization of the
334 LCI for particulate P, approximated as TP-SRP: as expected, the optimal (a,b) pairs lie in the same area
335 of parameter space as for TP (Fig 4).

336 Statistical approaches in catchment research often risk finding spurious correlations (Casquin et al.,
337 2021; Guillemot et al., 2021). Here, the fact that optimal (a, b) pairs for nitrate, SRP and TP agreed with
338 knowledge on their transfer pathways increases our confidence that the correlation represent mechanistic
339 associations and the CSA map derived from these correlations (Figure 5) could be used for management
340 purposes. Of course, correlations between the optimized LCI and flow-weighted mean P concentrations
341 remain modest ($r=0.56$ and 0.61 for SRP and TP, respectively), as several factors not included in the
342 LCI have an influence: point sources, characteristics of cropping systems, soil properties, etc. (Frei et
343 al., 2020; Guillemot et al., 2021).



344

345 **Figure 4. Optimization of the landscape configuration index (LCI) for (a) flow-weighted mean**
 346 **nitrate, (b) SRP and (c) TP. Black dots represent the top 50 optimal (a, b) pairs to examine**
 347 **uncertainty in parameter estimation.**



348

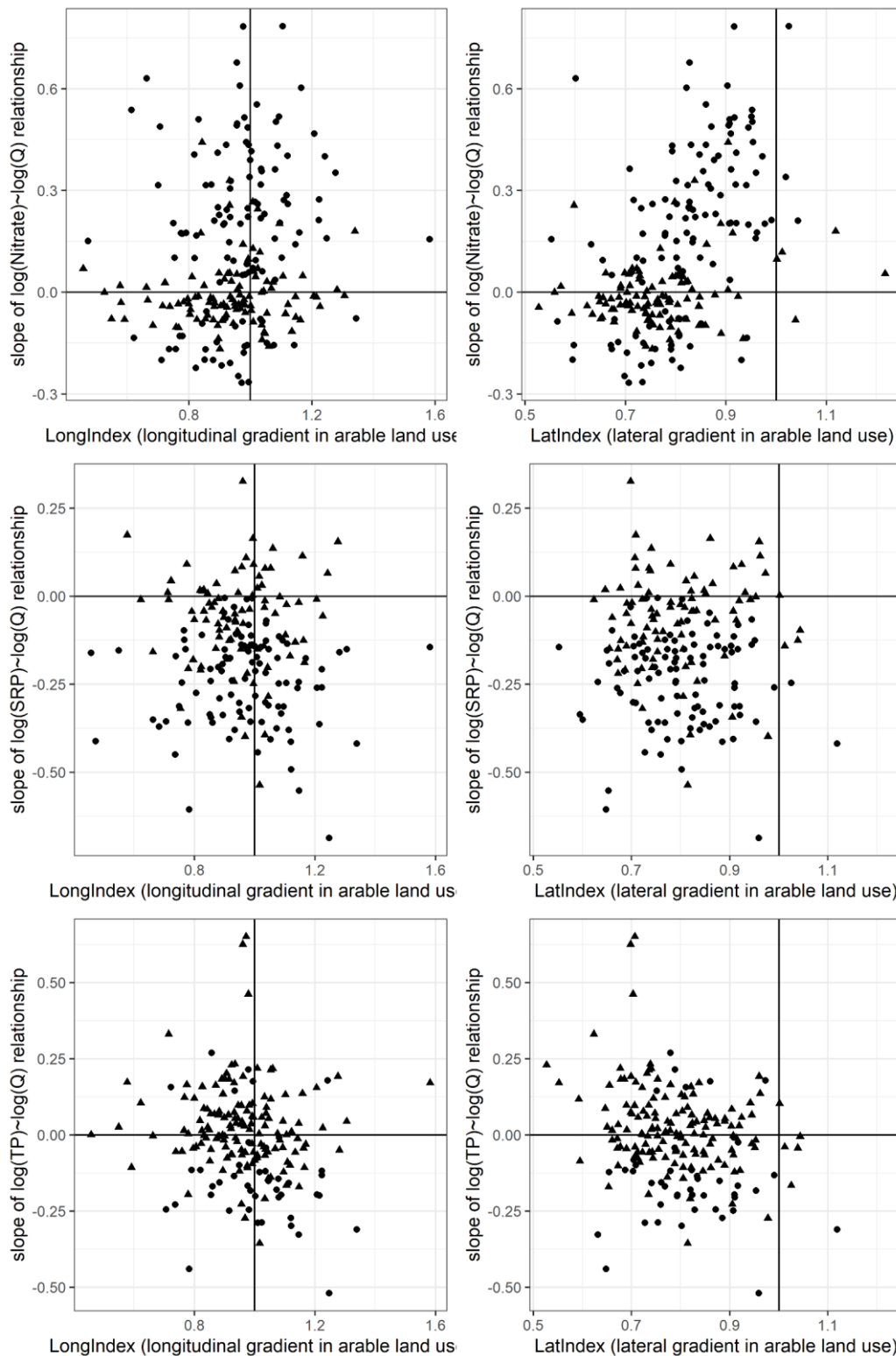
349 **Figure 5. Example of mapping critical source area (red) for (a) soluble reactive phosphorus and**
 350 **(b) total phosphorus (b) for one subcatchment in the study area.**

351 **3.3. Relationships between longitudinal and lateral distribution of arable land and**
 352 **concentration dynamics**

353 We investigated the influence of landscape spatial configuration on nitrate, SRP and TP concentration
 354 dynamics by examining correlations between indices of longitudinal and lateral distributions of arable
 355 land and the slope of the $\log(\text{concentration})$ - $\log(\text{discharge})$ relationship. Contrary to our hypothesis,
 356 none of the six relationships was significantly negative ($p > 0.05$), suggesting that the spatial distribution
 357 of nutrient sources in the longitudinal and lateral dimensions did not significantly influence
 358 concentration dynamics (Figure 6). This contradicts recent modelling (Musolff et al., 2017) or
 359 observational studies based on a few catchments (Dupas et al., 2021; Knapp et al., 2022) that suggested
 360 that lateral and longitudinal distributions of sources influenced concentration dynamics. It does support,
 361 however, most studies, which assume that vertical concentration gradients are the main factors that
 362 control concentration-discharge relationships (Botter et al., 2020; Ebeling et al., 2021b; Stewart et al.,
 363 2022). Although the vertical dimension showed higher nitrate concentrations in the subsurface in most
 364 situations (e.g. Stewart et al. (2022)), higher concentrations in deeper groundwater were also observed
 365 in research catchments in Brittany, resulting in negative nitrate concentration-discharge relationships
 366 (Martin et al., 2004; Ruiz et al., 2002). According to these studies, these “reverse” gradients can occur

367 when the catchments are on a path of recovery, as the deeper groundwater is more contaminated than
368 the younger shallow groundwater. In addition to spatial gradients of nutrient sources, in- and near-stream
369 processes can alter land-to-stream temporal dynamics via retention and remobilization processes, which
370 may mask effects of landscape spatial configuration (Casquin et al., 2020; Jarvie et al., 2011).

371 Relationships between the C-Q slope, lithology and the 10th percentile of discharge (Fig S4), suggest
372 that the supply of water during low flow and biogeochemical transformations has a key influence on the
373 seasonal dynamics of nitrates as captured by the log(concentration)-log(discharge) slope. Previous
374 research shows that the P concentration dynamics captured with low-resolution data were controlled
375 mainly by in-stream retention/remobilization processes and the degree of dilution of point sources, even
376 when the point sources represent a small fraction of annual loads (Abbott et al., 2018b; Casquin et al.,
377 2020; Dupas et al., 2018). Therefore, we conclude that landscape spatial configuration does not control
378 riverine nutrient dynamics more than the other factors previously identified in the literature.



379

380 **Figure 6. Relationships between the longitudinal and lateral distribution of arable land and**
 381 **nitrate, soluble reactive phosphorus (SRP) and total phosphorus (TP) concentration dynamics.**
 382 **Round dots indicate significant C-Q slope ($p < 0.05$) and triangular dots non-significant C-Q slopes**
 383 **($p > 0.05$).**

384 **4. Conclusion**

385 This study investigated the influence of the landscape spatial configuration on nitrate, SRP and TP mean
386 flow-weighted mean concentrations and seasonal dynamics. We used public water quality and discharge
387 data from >200 small headwaters located within a relatively homogeneous region to limit the influence
388 of confounding factors besides landscape configuration. We found that studying small (<50 km²)
389 headwater catchments led to inclusion of high variability in concentrations, landscape composition and
390 landscape organization. A landscape configuration index that included information on flow distance to
391 the stream and flow accumulation identified critical source areas for SRP and TP, but not nitrate. The
392 predominant influence of flow distance on SRP and flow accumulation on TP, and the lack of influence
393 of the landscape configuration on nitrate, is consistent with knowledge on the dominant transfer
394 pathways of these three nutrient forms. This increased our confidence that the correlation represents
395 mechanistic associations. The CSA maps created from this statistical analysis may thus help design
396 landscapes that minimize nutrient losses while maintaining arable land for crop production. For
397 example, one could relocate arable fields outside the CSAs, and widen the buffer strips or increase the
398 density of hedgerows within the CSAs. By contrast, the lateral and longitudinal distributions of arable
399 land did not seem to influence nutrient dynamics, which supports results of most previous studies, which
400 indicate that other factors such as vertical concentration gradients and the degree of dilution of point
401 sources have more influence. Future research on landscape and nutrient transfers should include a wider
402 variety of landscape elements, including linear elements such as ditches, hedgerows or other land uses,
403 while maintaining the simplicity of the parsimonious modelling framework used in this study.

404 **DATA AVAILABILITY**

405 The data and R scripts used in this paper are provided in the supplementary information.

406 **5. References**

- 407 Abbott, B.W. et al., 2018a. Unexpected spatial stability of water chemistry in headwater stream
408 networks. *Ecology Letters*, 21(2): 296-308.
- 409 Abbott, B.W. et al., 2018b. Trends and seasonality of river nutrients in agricultural catchments: 18 years
410 of weekly citizen science in France. *Science of the Total Environment*, 624: 845-858.
- 411 Basu, N.B. et al., 2010. Nutrient loads exported from managed catchments reveal emergent
412 biogeochemical stationarity. *Geophysical Research Letters*, 37.
- 413 Bernhardt, E.S. et al., 2017. Control Points in Ecosystems: Moving Beyond the Hot Spot Hot Moment
414 Concept. *Ecosystems*, 20(4): 665-682.

415 Berthier, L. et al., 2014. Enveloppes des milieux potentiellement humides de la France métropolitaine.
416 . Ministère d'Ecologie, du Développement Durable et de l'Énergie.: 50.

417 Betton, C., Webb, B.W., Walling, D.E., 1991. RECENT TRENDS IN NO₃-N CONCENTRATION
418 AND LOADS IN BRITISH RIVERS, Symp at the 20th General Assembly of the International
419 Union of Geodesy and Geophysics - Sediment and Stream Water Quality in a Changing
420 Environment. Iahs Publication, Vienna, Austria, pp. 169-180

421 Beven, K.J., Kirkby, M.J., 1979. A physically based, variable contributing area model of basin
422 hydrology / Un modèle à base physique de zone d'appel variable de l'hydrologie du bassin
423 versant. Hydrological Sciences Bulletin, 24(1): 43-69.

424 Bishop, K. et al., 2008. Aqua Incognita: the unknown headwaters. Hydrol. Process., 22(8): 1239-1242.

425 Bol, R. et al., 2018. Challenges of Reducing Phosphorus Based Water Eutrophication in the Agricultural
426 Landscapes of Northwest Europe. Frontiers in marine science, 5(276).

427 Botter, M., Li, L., Hartmann, J., Burlando, P., Fatichi, S., 2020. Depth of Solute Generation Is a
428 Dominant Control on Concentration-Discharge Relations. Water Resour. Res., 56(8).

429 Casal, L. et al., 2018. Optimal location of set-aside areas to reduce nitrogen pollution: a modelling study.
430 Journal of Agricultural Science, 156(9): 1090-1102.

431 Casquin, A. et al., 2021. The influence of landscape spatial configuration on nitrogen and phosphorus
432 exports in agricultural catchments. Landsc. Ecol., 36(12): 3383-3399.

433 Casquin, A. et al., 2020. River network alteration of C-N-P dynamics in a mesoscale agricultural
434 catchment. Science of the Total Environment, 749.

435 Covino, T., Riveros-Iregui, D.A., Schneider, C.L., 2022. 6.04 - Geomorphology Imparts Spatial
436 Organization on Hydrological and Biogeochemical Fluxes. In: Shroder, J.F. (Ed.), Treatise on
437 Geomorphology (Second Edition). Academic Press, Oxford, pp. 53-67.

438 de Lavenne, A., Cudennec, C., 2019. Assessment of freshwater discharge into a coastal bay through
439 multi-basin ensemble hydrological modelling. Science of the Total Environment, 669: 812-820.

440 Djodjic, F., Bierozza, M., Bergstrom, L., 2021. Land use, geology and soil properties control nutrient
441 concentrations in headwater streams. Science of the Total Environment, 772.

442 Djodjic, F., Markensten, H., 2019. From single fields to river basins: Identification of critical source
443 areas for erosion and phosphorus losses at high resolution. Ambio, 48(10): 1129-1142.

444 Djodjic, F., Villa, A., 2015. Distributed, high-resolution modelling of critical source areas for erosion
445 and phosphorus losses. Ambio, 44: S241-S251.

446 Doody, D.G. et al., 2016. Optimizing land use for the delivery of catchment ecosystem services.
447 Frontiers in Ecology and the Environment, 14(6): 325-332.

448 Dorioz, J.M., Wang, D., Poulenard, J., Trevisan, D., 2006. The effect of grass buffer strips on
449 phosphorus dynamics - A critical review and synthesis as a basis for application in agricultural
450 landscapes in France. Agriculture Ecosystems & Environment, 117(1): 4-21.

451 Dupas, R., Causse, J., Jaffrezic, A., Aquilina, L., Durand, P., 2021. Flowpath controls on high-spatial-
452 resolution water-chemistry profiles in headwater streams. Hydrol. Process., 35(6).

453 Dupas, R. et al., 2013. Assessing N emissions in surface water at the national level: comparison of
454 country-wide vs. regionalized models. Sci Total Environ, 443: 152-62.

455 Dupas, R., Ehrhardt, S., Musolff, A., Fovet, O., Durand, P., 2020. Long-term nitrogen retention and
456 transit time distribution in agricultural catchments in western France. Environmental Research
457 Letters.

458 Dupas, R., Gascuel-Oudou, C., Gilliet, N., Grimaldi, C., Gruau, G., 2015. Distinct export dynamics for
459 dissolved and particulate phosphorus reveal independent transport mechanisms in an arable
460 headwater catchment. Hydrol. Process., 29(14): 3162-3178.

461 Dupas, R. et al., 2017. The role of mobilisation and delivery processes on contrasting dissolved nitrogen
462 and phosphorus exports in groundwater fed catchments. Science of the Total Environment(599-
463 600): 1275–1287.

464 Dupas, R., Minaudo, C., Gruau, G., Ruiz, L., Gascuel-Oudou, C., 2018. Multidecadal trajectory of
465 riverine nitrogen and phosphorus dynamics in rural catchments. Water Resour. Res., 54: 5327–
466 5340.

467 Ebeling, P. et al., 2021a. Long-Term Nitrate Trajectories Vary by Season in Western European
468 Catchments. Global Biogeochemical Cycles, 35(9).

469 Ebeling, P. et al., 2021b. Archetypes and Controls of Riverine Nutrient Export Across German
470 Catchments. *Water Resour. Res.*, 57(4).

471 Ehrhardt, S. et al., 2021. Nitrate Transport and Retention in Western European Catchments Are Shaped
472 by Hydroclimate and Subsurface Properties. *Water Resour. Res.*, 57(10).

473 Fovet, O. et al., 2018. Seasonal variability of stream water quality response to storm events captured
474 using high-frequency and multi-parameter data. *Journal of Hydrology*, 559: 282-293.

475 Frei, R.J. et al., 2020. Predicting Nutrient Incontinence in the Anthropocene at Watershed Scales.
476 *Frontiers in Environmental Sciences*, 7: 200.

477 Godsey, S.E., Hartmann, J., Kirchner, J.W., 2019. Catchment chemostasis revisited: Water quality
478 responds differently to variations in weather and climate. *Hydrol. Process.*, 33(24): 3056-3069.

479 Gu, S. et al., 2021. Spatial Persistence of Water Chemistry Patterns Across Flow Conditions in a
480 Mesoscale Agricultural Catchment. *Water Resour. Res.*, 57(7).

481 Gu, S. et al., 2017. Release of dissolved phosphorus from riparian wetlands: evidence for complex
482 interactions among hydroclimate variability, topography and soil properties. *Science of the*
483 *Total Environment*(598): 421–431.

484 Guillemot, S. et al., 2021. Spatio-temporal controls of C-N-P dynamics across headwater catchments of
485 a temperate agricultural region from public data analysis. *HESSD*.

486 Jarvie, H.P. et al., 2011. Quantifying Phosphorus Retention and Release in Rivers and Watersheds Using
487 Extended End-Member Mixing Analysis (E-EMMA). *Journal of Environmental Quality*, 40(2):
488 492-504.

489 Jencso, K.G. et al., 2009. Hydrologic connectivity between landscapes and streams: Transferring reach-
490 and plot-scale understanding to the catchment scale. *Water Resour. Res.*, 45.

491 Knapp, J.L.A., Li, L., Musolff, A., 2022. Hydrologic connectivity and source heterogeneity control
492 concentration-discharge relationships. *Hydrol. Process.*, 36(9).

493 Krause, S. et al., 2017. Ecohydrological interfaces as hot spots of ecosystem processes. *Water Resour.*
494 *Res.*, 53(8): 6359-6376.

495 Lane, S.N., Reaney, S.M., Heathwaite, A.L., 2009. Representation of landscape hydrological
496 connectivity using a topographically driven surface flow index. *Water Resour. Res.*, 45(8): n/a-
497 n/a.

498 Le Moal, M. et al., 2019. Eutrophication: A new wine in an old bottle. *Science of The Total*
499 *Environment*, 651: 1-11.

500 Legeay, P.-L., Gruau, G., 2014. Spatio-temporal analysis of phosphorus fluxes and sources in Breton
501 rivers. *Trans-P project*.

502 Liu, S. et al., 2022. Controls on Spatial Variability in Mean Concentrations and Export Patterns of River
503 Chemistry Across the Australian Continent. *Water Resour. Res.*, 58(e2022WR032365).

504 Lutz, S.R. et al., 2020. How Important is Denitrification in Riparian Zones? Combining End-Member
505 Mixing and Isotope Modeling to Quantify Nitrate Removal from Riparian Groundwater. *Water*
506 *Resour. Res.*, 56(1).

507 Martin, C. et al., 2004. Seasonal and interannual variations of nitrate and chloride in stream waters
508 related to spatial and temporal patterns of groundwater concentrations in agricultural
509 catchments. *Hydrol. Process.*, 18(7): 1237-1254.

510 McDowell, R.W. et al., 2014. Contrasting the spatial management of nitrogen and phosphorus for
511 improved water quality: Modelling studies in New Zealand and France. *European Journal of*
512 *Agronomy*, 57: 52-61.

513 McDowell, R.W., Srinivasan, M.S., 2009. Identifying critical source areas for water quality: 2.
514 Validating the approach for phosphorus and sediment losses in grazed headwater catchments.
515 *Journal of Hydrology*, 379(1-2): 68-80.

516 Mellander, P.E., Jordan, P., Shore, M., Melland, A.R., Shortle, G., 2015. Flow paths and phosphorus
517 transfer pathways in two agricultural streams with contrasting flow controls. *Hydrol. Process.*

518 Minaudo, C. et al., 2019. Seasonal and event-based concentration-discharge relationships to identify
519 catchment controls on nutrient export regimes. *Advances in Water Resources*.

520 Moatar, F., Abbott, B.W., Minaudo, C., Curie, F., Pinay, G., 2017. Elemental properties, hydrology, and
521 biology interact to shape concentration-discharge curves for carbon, nutrients, sediment, and
522 major ions. *Water Resour. Res.*, 53(2): 1270-1287.

523 Musolff, A., Fleckenstein, J.H., Rao, P.S.C., Jawitz, J.W., 2017. Emergent archetype patterns of coupled
524 hydrologic and biogeochemical responses in catchments. *Geophysical Research Letters*, 44(9):
525 4143-4151.

526 Musolff, A., Schmidt, C., Selle, B., Fleckenstein, J.H., 2015. Catchment controls on solute export.
527 *Advances in Water Resources*, 86: 133-146.

528 Musolff, A. et al., 2021. Spatial and Temporal Variability in Concentration-Discharge Relationships at
529 the Event Scale. *Water Resour. Res.*, 57(10).

530 Peterson, E.E., Sheldon, F., Darnell, R., Bunn, S.E., Harch, B.D., 2011. A comparison of spatially
531 explicit landscape representation methods and their relationship to stream condition. *Freshw.*
532 *Biol.*, 56(3): 590-610.

533 Pionke, H.B., Gburek, W.J., Schnabel, R.R., Sharpley, A.N., Elwinger, G.F., 1999. Seasonal flow,
534 nutrient concentrations and loading patterns in stream flow draining an agricultural hill-land
535 watershed. *Journal of Hydrology*, 220(1-2): 62-73.

536 Qin, C. et al., 2007. An adaptive approach to selecting a flow-partition exponent for a multiple-flow-
537 direction algorithm. *International Journal of Geographical Information Science*, 21(4): 443-458.

538 Reaney, S.M. et al., 2019. Identifying critical source areas using multiple methods for effective diffuse
539 pollution mitigation. *Journal of Environmental Management*, 250.

540 R Core Team (202). R: A language and environment for statistical computing. R Foundation for
541 Statistical Computing, Vienna, Austria. URL <https://www.R-project.org/>

542 Ruiz, L. et al., 2002. Effect on nitrate concentration in stream water of agricultural practices in small
543 catchments in Brittany : II. Temporal variations and mixing processes. *Hydrology and Earth*
544 *System Sciences*, 6(3): 507-513.

545 Schoumans, O.F. et al., 2014. Mitigation options to reduce phosphorus losses from the agricultural sector
546 and improve surface water quality: A review. *Science of the Total Environment*, 468: 1255-
547 1266.

548 Shogren, A.J. et al., 2019. Revealing biogeochemical signatures of Arctic landscapes with river
549 chemistry. *Scientific Reports*, 9.

550 Shore, M. et al., 2014. Evaluating the critical source area concept of phosphorus loss from soils to water-
551 bodies in agricultural catchments. *Science of the Total Environment*, 490: 405-415.

552 Stamm, C., Jarvie, H.P., Scott, T., 2014. What's More Important for Managing Phosphorus: Loads,
553 Concentrations or Both? *Environmental Science & Technology*, 48(1): 23-24.

554 Staponites, L.R., Bartak, V., Bily, M., Simon, O.P., 2019. Performance of landscape composition
555 metrics for predicting water quality in headwater catchments. *Scientific Reports*, 9.

556 Stewart, B. et al., 2022. Streams as Mirrors: Reading Subsurface Water Chemistry From Stream
557 Chemistry. *Water Resour. Res.*, 58(1).

558 Strohmenger, L., Fovet, O., Hrachowitz, M., Salmon-Monviola, J., Gascuel-Oudou, C., 2021. Is a simple
559 model based on two mixing reservoirs able to reproduce the intra-annual dynamics of DOC and
560 NO₃ stream concentrations in an agricultural headwater catchment? *Science of the Total*
561 *Environment*, 794.

562 Team, R.C., 2021. R: A language and environment for statistical computing. R Foundation for Statistical
563 Computing, Vienna, Austria.

564 Thomas, I.A. et al., 2016. A sub-field scale critical source area index for legacy phosphorus management
565 using high resolution data. *Agriculture Ecosystems & Environment*, 233: 238-252.

566 Thompson, S.E., Basu, N.B., Lascrain, J., Jr., Aubeneau, A., Rao, P.S.C., 2011. Relative dominance of
567 hydrologic versus biogeochemical factors on solute export across impact gradients. *Water*
568 *Resour. Res.*, 47.

569 Van Meter, K.J., Chowdhury, S., Byrnes, D.K., Basu, N.B., 2020. Biogeochemical asynchrony:
570 Ecosystem drivers of seasonal concentration regimes across the Great Lakes Basin. *Limnology*
571 *and Oceanography*, 65(4): 848-862.

572 Van Sickle, J., Johnson, C.B., 2008. Parametric distance weighting of landscape influence on streams.
573 *Landsc. Ecol.*, 23(4): 427-438.

574 Walsh, C.J., Webb, J.A., 2014. Spatial weighting of land use and temporal weighting of antecedent
575 discharge improves prediction of stream condition. *Landsc. Ecol.*, 29(7): 1171-1185.

576 Winter, C. et al., 2021. Disentangling the Impact of Catchment Heterogeneity on Nitrate Export
577 Dynamics From Event to Long-Term Time Scales. *Water Resour. Res.*, 57(1).

578 Zampella, R.A., Procopio, N.A., Lathrop, R.G., Dow, C.L., 2007. Relationship of land-use/land-cover
579 patterns and surface-water quality in the Mullica River basin. *Journal of the American Water*
580 *Resources Association*, 43(3): 594-604.

581 Zarnetske, J.P., Bouda, M., Abbott, B.W., Saiers, J., Raymond, P.A., 2018. Generality of Hydrologic
582 Transport Limitation of Watershed Organic Carbon Flux Across Ecoregions of the United States
583 *Geophysical Research Letters*.

584 Zimmer, M.A., McGlynn, B.L., 2018. Lateral, Vertical, and Longitudinal Source Area Connectivity
585 Drive Runoff and Carbon Export Across Watershed Scales. *Water Resour. Res.*, 54(3): 1576-
586 1598.

587

588 **SUPPORTING INFORMATION: Landscape spatial configuration influences**
589 **phosphorus but not nitrate concentrations in agricultural headwater**
590 **catchments**

591 Rémi Dupas ¹, Antoine Casquin ², Patrick Durand ¹, Valérie Viaud ¹

592 ¹ INRAE, UMR SAS 1069, L'Institut Agro, Rennes, France

593 ² Sorbonne Université - UPMC, UMR METIS, Paris, France

594

595 **Corresponding Author:** Rémi Dupas, remi.dupas@inrae.fr

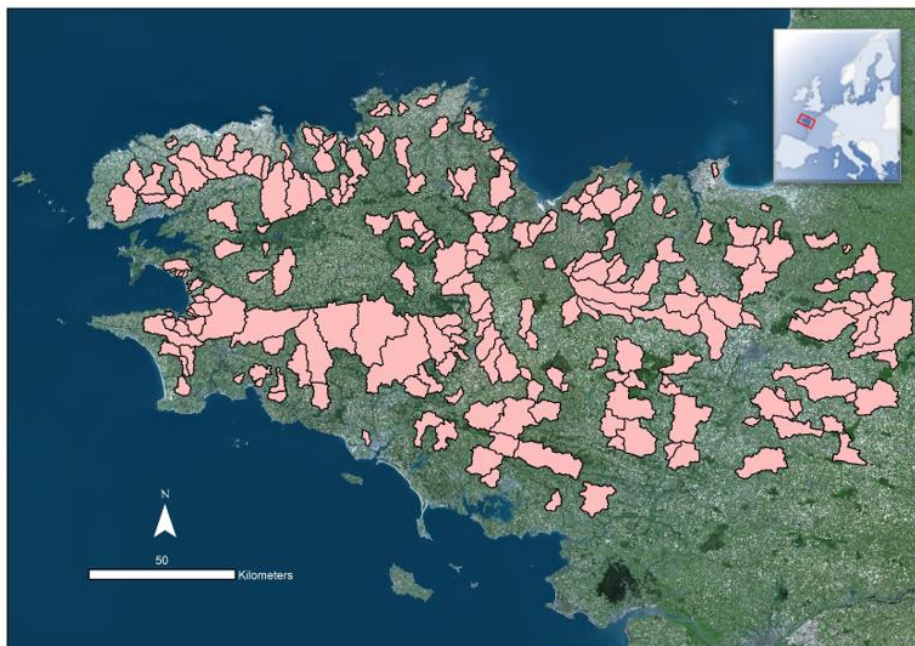
596

597 The R code to compute the Landscape Configuration Index is provided in a .zip file.

598 Table S1. Catchment properties

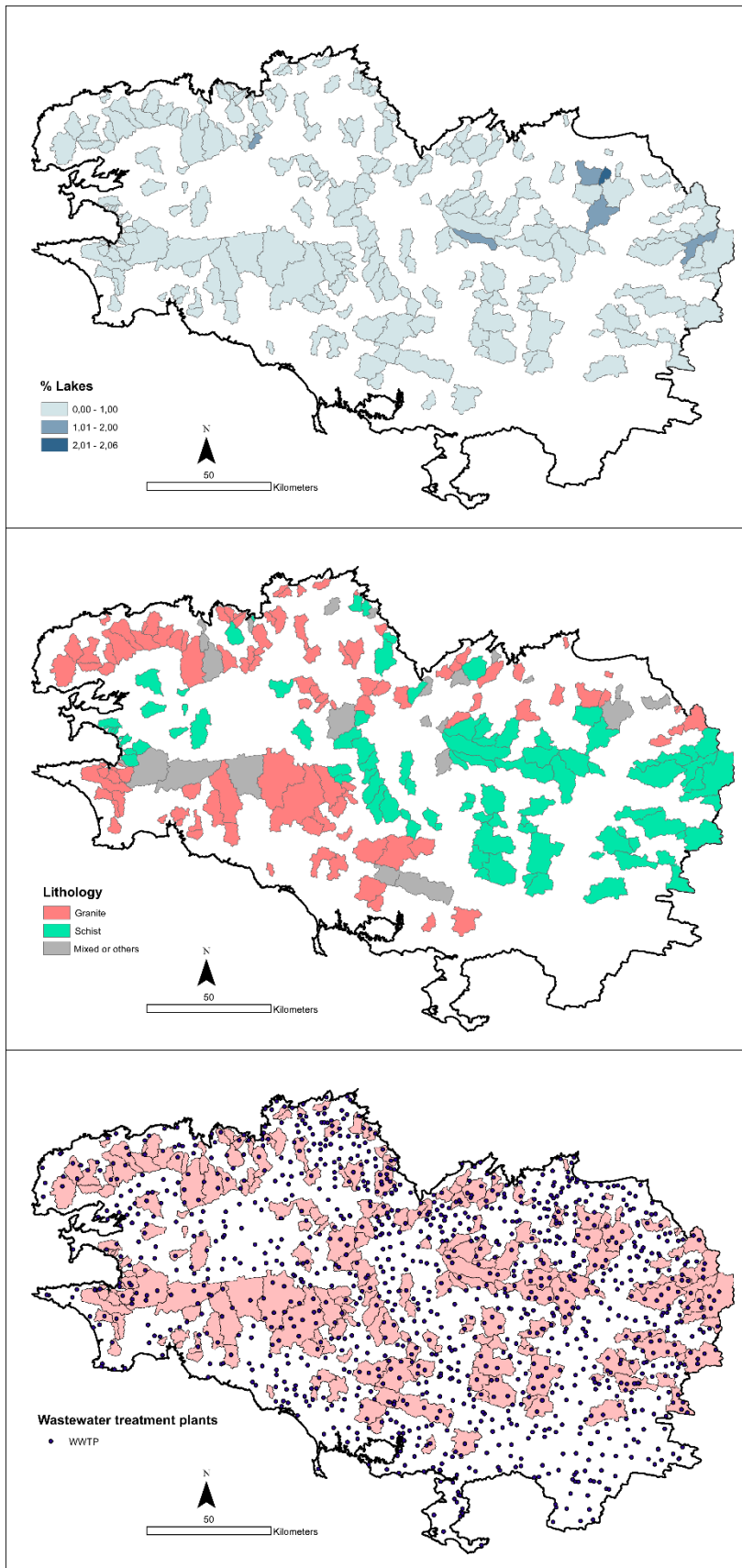
	surface area (km ²)	annual runoff (mm)	10% percentile discharge (mm/day)	of %arable land use
minimum	1	163	0	3
1st quartile	16	263	0.05	44
median	30	403	0.13	53
mean	47	436	0.17	51
3rd quartile	60	593	0.25	59
max	300	878	0.62	76

599



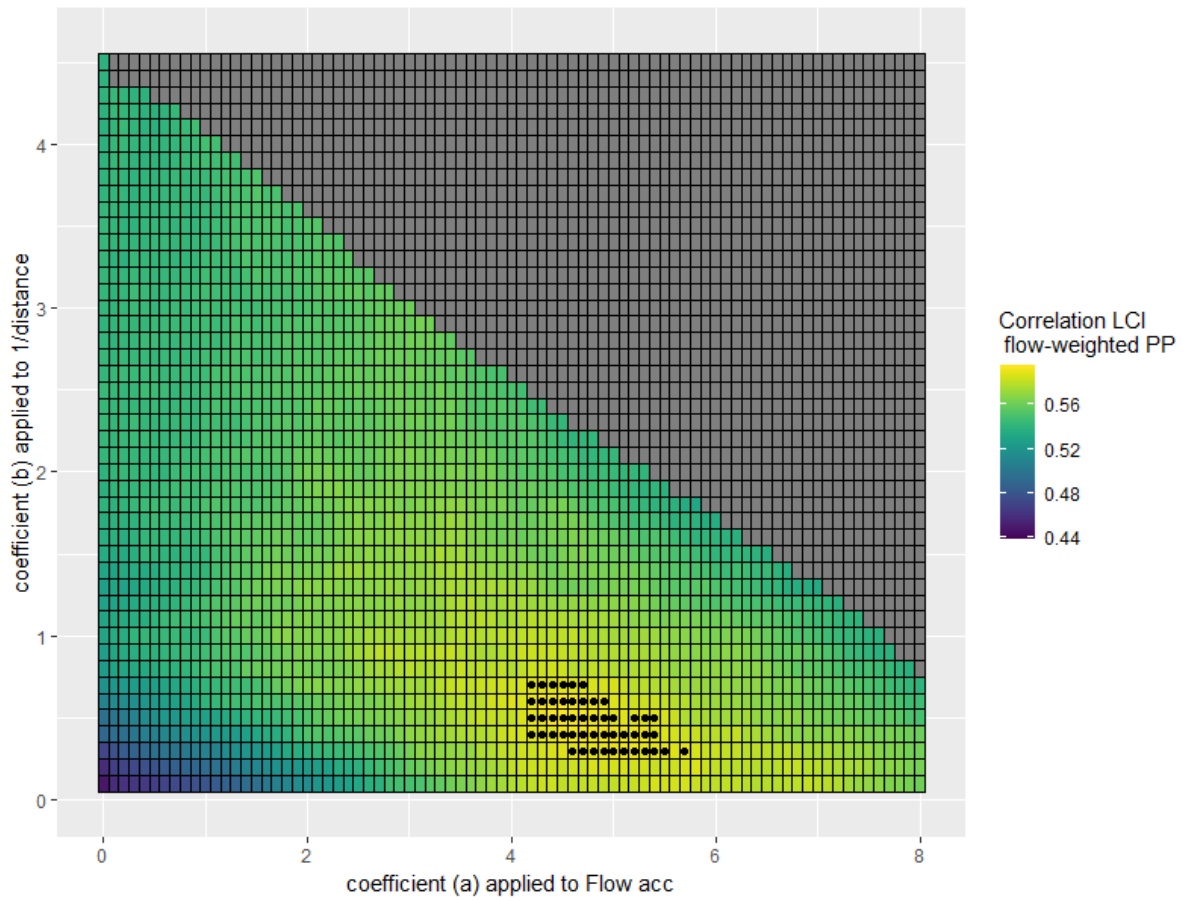
600

601 Figure S1. Location of the 221 study catchments in the Brittany region (western France).



602

603 Figure S2. Additional catchments properties: percentage of the catchment area covered by lakes, main
 604 lithology and location of wastewater treatment plants.

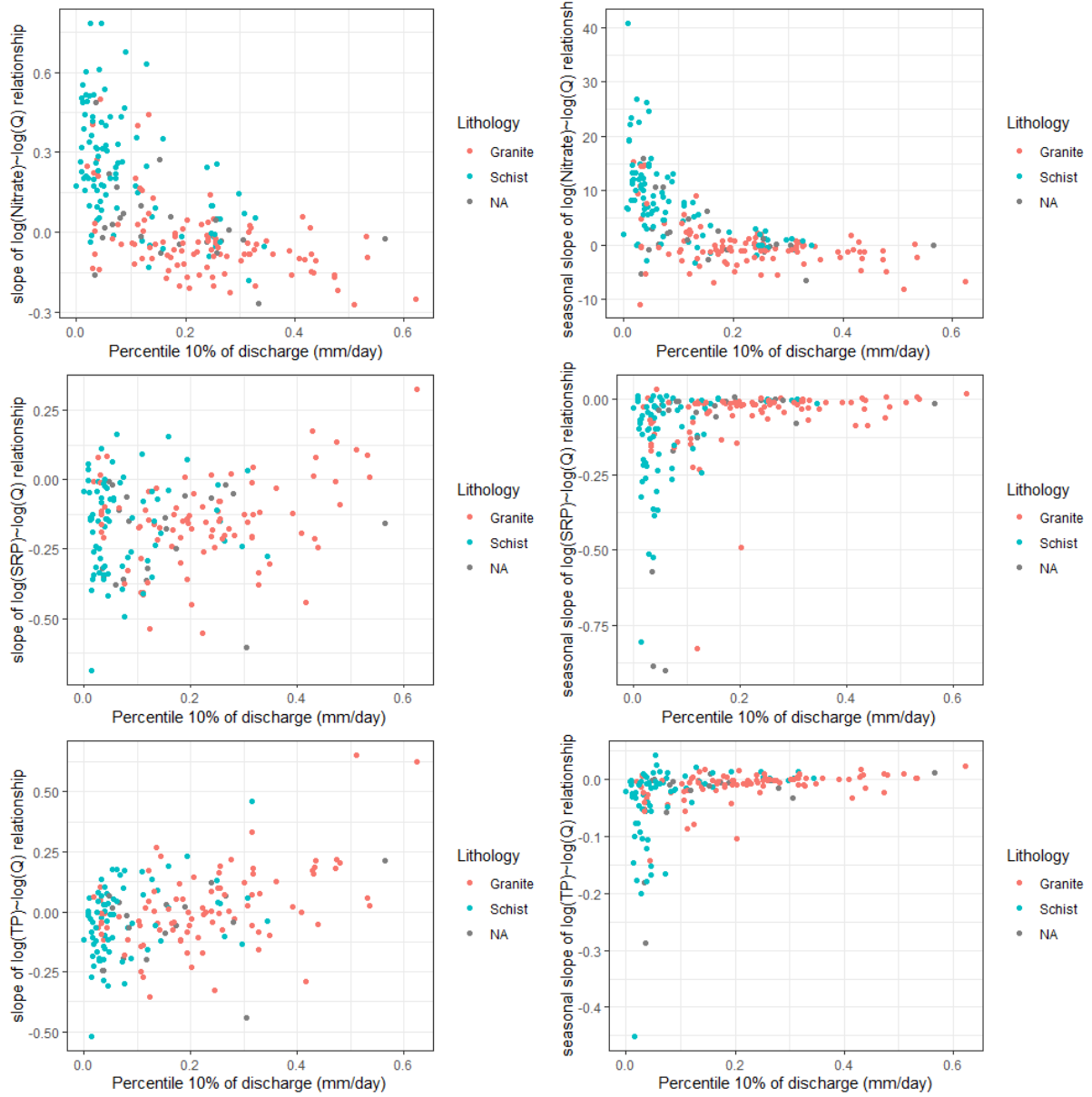


605

606 Figure S3. Optimization of the landscape configuration index (LCI) for particulate phosphorus PP,
 607 estimated as TP-SRP. Black dots represent the top 50 optimal (a, b) pairs to examine uncertainty in
 608 parameter estimation.

609

610



611

612 Figure S4. Relationships between the slope of the log(concentration)-log(discharge) slope and
 613 catchments variables: dominant lithology class and percentile 10% of discharge.

614

615

616

617